

## ARTICLE

## FRET based ratiometric switch for selective sensing of Al<sup>3+</sup> with bio-imaging in human peripheral blood mononuclear cells PBMCs

Sangita Das<sup>a\*</sup>, Partha Pratim Das<sup>b</sup>, James W. Walton<sup>a</sup>, Kakali Ghoshal<sup>c</sup>, Lakshman Patra<sup>d</sup> and Maitree Bhattacharyya<sup>c</sup>

Received 00th January 20xx,  
Accepted 00th January 20xx

DOI: 10.1039/x0xx00000x

In this paper, triphenylamine and rhodamine-B (Donor-Acceptor) hybrid switch (TPRH) was rationally designed, synthesised and characterised as novel fluorescence resonance energy transfer (FRET) ratiometric fluorescent chemosensor for specific sensing of Al<sup>3+</sup> over other important metal ions in mixed aqueous solution. We proposed that the sensor in hand (TPRH) is non-toxic and can be successfully employed as Al<sup>3+</sup> triggered intracellular 'FRET-ON' mechanism. The orientation of the probe was designed in such a way that fluorescence (or Förster) resonance energy transfer (FRET) mechanism was operated from the 'donor moiety' Triphenylamine to 'accepter moiety' rhodamine-B. This fluorescent probe was found to be highly selective towards Al<sup>3+</sup> over other important guest metal ions, including Fe<sup>3+</sup> and Cr<sup>3+</sup>. Considering the adverse effect of Al<sup>3+</sup> ions on human health and also in the environment, there is great value to the development of sensitive and specific tools for the detection of Al<sup>3+</sup> ions. The limit of detection (LOD) of TPRH was found to be in the order of 10<sup>-8</sup> M. The TPRH-Al<sup>3+</sup> complex showed reversible binding with demetallation in presence of EDTA anion. In accordance with this reversibility, the fluorescence output at 576 nm from two active chemical inputs, namely Al<sup>3+</sup> and EDTA followed a truth table of an INHIBIT logic gate. To show applicability, TPRH was shown to be able to detect and analyze Al<sup>3+</sup> at trace levels in various different water sources. Moreover, cytotoxic study found the probe was safe to use in a biological system with good cell membrane permeability. More importantly, bio-imaging of living human peripheral blood mononuclear cells (PBMCs) showed that TPRH could be used as an effective fluorescent probe for a prominent ratiometric in-vitro detection of transition trivalent metal ion Al<sup>3+</sup>. We evidenced a significant ( $p < 0.05$ ) shifts from blue (401 ± 117.7) to red (2851 ± 511.6) fluorescence when Al<sup>3+</sup> was added in the cell suspension, thus proving TPRH being a good candidate to detect intracellular Al<sup>3+</sup>.

### Introduction

Recently, the selective and sensitive detection of metal ions with smart fluorescence tools have attracted significant attention.<sup>1-7</sup> Metal ions play varied and important roles in living organisms as well as in the environment. These roles are often directly related to human health and global pollution problems. Hence, there is a great need to develop innovative chemosensor tools for monitoring concentrations of these ions. Aluminium is the third most abundant element in the Earth's crust. It is a nonessential metal for bio-organisms and has significant toxicity. Aluminium salts are neurotoxic and have been associated with Parkinson's disease<sup>8</sup> and Alzheimer's disease.<sup>9</sup> Furthermore, Al<sup>3+</sup> has been shown to lead to break in the DNA double-strand and to inhibit the repair of radiation-induced lesions in human peripheral blood lymphocytes.<sup>10</sup> It was also found that chronic exposure to Al<sup>3+</sup> can be extremely damaging

to patients with renal dysfunction.<sup>11</sup> Aluminium is widely used in our daily lives within electrical devices, building materials, food packaging, drinking water supplies and cookware. The widespread use of aluminium increases the likelihood of its release into the environment<sup>12</sup> and of exposure of humans and animals, through food and water contamination. The concentration of aluminium in natural waters can vary significantly depending on various physicochemical and mineralogical factors. According to the World Health Organisation, the threshold limit of Al<sup>3+</sup> in drinking water is 7.41 μM and the daily intake of aluminium should be less than 3–10 mg.<sup>13</sup> It is clear that, due to the hazardous potential of aluminium, the development of tools to detect trace levels of Al<sup>3+</sup> is of paramount importance.

The gold standard in fluorescence sensing is ratiometric analysis of two wavelengths, which allows for sensing of analytes without needing to know the concentration of the probe and overcomes issues of quenching of emission by exogenous species. There are several examples of non-ratiometric fluorescence and colorimetric Al<sup>3+</sup> sensors, which undergo spectroscopic changes upon metal binding.<sup>14</sup> Improved sensors, which give ratiometric response to Al<sup>3+</sup> have been reported, but most of them suffer from either a pH

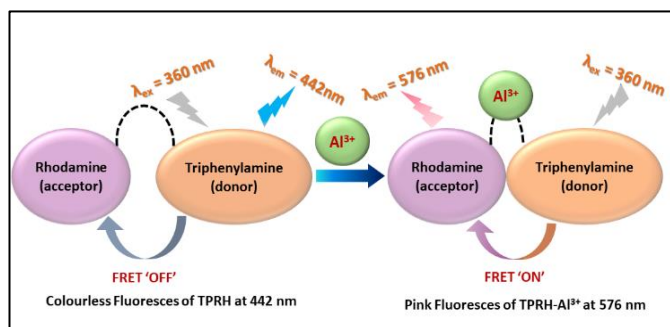
<sup>a</sup> Durham University, Department of Chemistry, Durham, DH1 3LE, UK, Email: sangita.das@durham.ac.uk

<sup>b</sup> Department of Earth System Sciences, Yonsei University, Seoul 120749, Korea

<sup>c</sup> Department of Biochemistry, University of Calcutta, 35 Ballygunge Circular Road, Kolkata 700019, India

<sup>d</sup> Department of Chemistry, Jadavpur University, Jadavpur, Kolkata, India.

dependence<sup>15</sup> or a lack of selectivity over other ions<sup>16</sup> but FRET based ratiometric bio-imaging is rare.<sup>17</sup> FRET is a non-radiative process, in which excited state energy transfer was operated from donor fluorophore to acceptor fluorophore through dipole-dipole interactions and/or multipolar interaction.



**Scheme 1:** TPRH sensing of Al<sup>3+</sup> via a FRET mechanism.

FRET containing potent molecular switch are extremely sensible in cell physiology, fast reaction time, optical therapy and more importantly ultra-sensitive sensing in molecules and/or ionic species.<sup>18</sup> Fluorescent switches which can instantaneously recognise biologically and environmentally important ions by fluorescence imaging have become essential implements in various fields of medical and chemical science.<sup>19</sup> In this regard, fluorescence chemosensors provide significant advantages due to their high sensitivity, specificity and prompt response for real-time monitoring the activities of guest analyt inside living cells.<sup>20</sup> However, it is a prime requirement to study the bio-imaging mechanism by using small FRET molecular fluorophore that describes aluminium ions cause aluminium-induced human diseases. In this aspect, rhodamine-based compounds are gaining considerable interest for cell imaging applications, due to their unique change in fluorescence emission with spiroactam ring opening after addition of guest cation.<sup>21</sup> FRET based triphenylamine-rhodamine blended probe which can specifically detect intracellular Al<sup>3+</sup> is extremely rare. So, keeping in view of recent chronic exposure of Al<sup>3+</sup> with it's significant toxicity, it is an urge demand to develop promising fluorescent tools which can selectively detect trace levels of Al<sup>3+</sup>. In continuation of our previous work on fluorescence sensors,<sup>22</sup> herein, a new rhodamine-triphenylamine-based FRET sensor, TPRH, has been designed, synthesised and characterised for the selective detection of Al<sup>3+</sup>.

We have designed the probe keeping in mind, that it will show FRET mechanism after selective binding with Al<sup>3+</sup> in mixed aqueous medium. For this mechanism to play well, we have chosen the donor portion (D) as triphenylamine and acceptor (A) as rhodamine, also added a linker ethylene diamine (ED), to make an arrangement D-ED-A. This architecture of the probe is responsible to make the binding site closer after interaction with Al<sup>3+</sup> and to initiate the FRET process ON.

TPRH exhibits a response in its UV absorption and fluorescence emission spectra upon addition of Al<sup>3+</sup>, with a limit of detection (LOD) of in the 10<sup>-8</sup> M concentration range and high selectivity towards Al<sup>3+</sup>. The bio-imaging experiments evidenced that TPRH

could successfully measure the Al<sup>3+</sup> that has been loaded in the cell suspension, without damaging the cells.

The response to Al<sup>3+</sup> likely arises from modulation of FRET between triphenylamine (donor) and rhodamine (acceptor) within the sensor framework (Scheme 1). The two emission peaks used for ratiometric analysis have a large difference in wavelength ( $\Delta\lambda = 134$  nm), which avoids any issues of interference. Al<sup>3+</sup> detection was possible in a variety of real-life water sources and a reversible INHIBIT logic gate was developed with two chemical inputs (Al<sup>3+</sup> and EDTA) and fluorescence output at 576 nm.

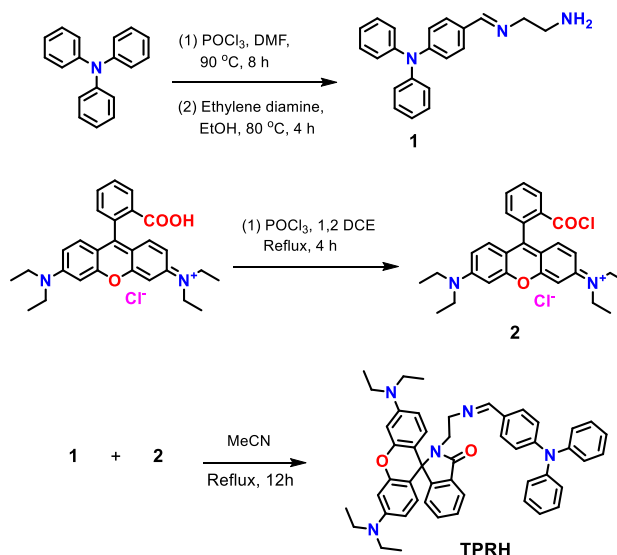
## Results and discussion

### Synthetic procedures

The synthetic route to TPRH is shown in Scheme 2. Triphenylamine was converted to 4-(diphenylamino) benzaldehyde according to a literature procedure,<sup>23</sup> before reaction with ethylene diamine afforded 4-(((2-aminoethyl)imino)methyl)-N,N-diphenylaniline (**1**). The rhodamine-derivative **2** was synthesised according to a literature procedure.<sup>24</sup> Reaction of intermediates **1** and **2** in refluxing acetonitrile gave the final probe, TPRH. Novel compounds **1** and **TPRH** were characterised by multinuclear NMR spectroscopy and HRMS (Figure S8 – S13, ESI).

### Photophysical studies

The effect of addition of various ions to a solution of TPRH was initially investigated by the naked eye, whereupon it was noted that addition of Al<sup>3+</sup> salts to the colourless TPRH solution led to an intense prominent red colouration. This result encouraged us to focus in detail on the sensing behaviour of TPRH towards Al<sup>3+</sup>.



**Scheme 2:** Synthesis of the receptor TPRH.

A series of photophysical studies were carried out, which included UV/Vis absorption and fluorescence emission titration,

along with selectivity and binding LOD studies. pH dependence and reversibility were also investigated. Furthermore, the new sensor was explored in a molecular logic gate application and as a potential solid state dip stick device to detect  $\text{Al}^{3+}$ . Finally, the sensor applicability was determined by sensing  $\text{Al}^{3+}$  in a wide range of water sources. Unless otherwise stated photophysical studies were carried out in a mixed methanol/aqueous solution (MeOH/ $\text{H}_2\text{O}$ , 1/4, v/v) of TPRH (20  $\mu\text{M}$ ), containing 10 mM HEPES buffer at pH 7.2 and 25  $^\circ\text{C}$ . Solutions of ionic salts (metal perchlorates or metal chlorides) were prepared in the same aqueous buffer at pH 7.2.

### UV-vis study

In the absence of any guest analytes, a solution of TPRH exhibits characteristic absorption bands at 275 nm and 352 nm. The absence of absorption at 550 nm indicates that the probe is stable in the solution phase in the closed spirolactam form. Upon incremental addition of a solution of  $\text{AlCl}_3$  (0–30  $\mu\text{M}$  final concentrations), the peaks at 275 nm and 352 nm gradually decrease and a new peak arises at 550 nm, which is characteristic of the opening of the spirolactam ring (Fig. 1a). The associated change in colour from colourless TPRH to a deep pink-red coloured solution was clearly visible by eye (Fig. 1a, inset). To investigate the selectivity of TPRH towards  $\text{Al}^{3+}$ , a selection of other guest metal ions (up to 5 equivalents) were titrated into a solution of TPRH. No other guest analytes exhibited notable changes in the UV-vis profile (Fig. 1b), including  $\text{Na}^+$ ,  $\text{K}^+$ ,  $\text{Ca}^{2+}$ ,  $\text{Mg}^{2+}$ ,  $\text{Fe}^{3+}$ ,  $\text{Co}^{2+}$ ,  $\text{Ni}^{2+}$ ,  $\text{Cu}^{2+}$ ,  $\text{Zn}^{2+}$ ,  $\text{Pb}^{2+}$ ,  $\text{Cd}^{2+}$ ,  $\text{Hg}^{2+}$ ,  $\text{Ni}^{2+}$ ,  $\text{Cr}^{3+}$  and  $\text{Mn}^{2+}$ . These results show that TPRH possesses excellent selectivity towards  $\text{Al}^{3+}$  and augurs well for its use as a highly specific colorimetric sensor.

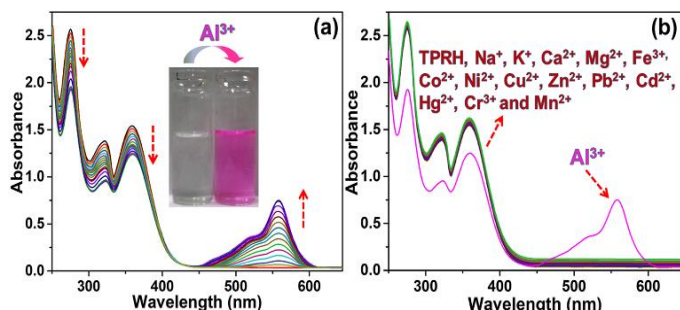


**Figure 1:** (a) UV-vis spectra of TPRH upon gradual addition of  $\text{Al}^{3+}$  (0 to 1.5 equivalents). (b) UV-vis spectra of TPRH upon addition of 5 equivalents of stated guest cations. TPRH (20  $\mu\text{M}$ ) in MeOH/ $\text{H}_2\text{O}$  (1/4, v/v), HEPES buffer (10 mM), pH 7.2, 25  $^\circ\text{C}$ .

This result is in contrast to many other  $\text{Al}^{3+}$  sensors, which typically show interference from other metal cations, particularly  $\text{Mn}^{2+}$ ,  $\text{Ca}^{2+}$ ,  $\text{Cr}^{3+}$  and  $\text{Fe}^{3+}$ . The addition of  $\text{Al}^{3+}$  to TPRH gives a linear response in the absorption intensity at 550 nm, with an  $R^2$  value of 0.998 (Fig. S1, ESI) and a limit of detection (LOD) of  $3.5 \times 10^{-8}$  M. An association constant ( $K_a$ ) of  $5.9 \times 10^5$   $\text{M}^{-1}$  was calculated, using the Benesi–Hildebrand equation (Fig S2, ESI).

### Fluorescence study

The response of TPRH to  $\text{Al}^{3+}$  was also investigated by fluorescence emission titration. In a similar way to the UV/Vis studies,  $\text{Al}^{3+}$  was titrated into a solution of TPRH and the

fluorescence emission measured, following excitation at 350 nm. In the absence of guest analyte, the free receptor gives a prominent emission signal at 442 nm from the triphenyl moiety and no peak at 576 nm, which indicates a stable spirolactam rhodamine B (Fig 2a). A photoluminescence quantum yield of  $\Phi = 0.21$  was calculated (see ESI). Upon incremental addition of  $\text{Al}^{3+}$  into the solution a reduction in emission intensity at 442 nm took place with the appearance of a new red-shifted peak at 576 nm (Fig. 2a). The resultant emission spectra reveal an isoemissive point at 547 nm and allows for ratiometric analysis by comparing peaks at 576 and 442 nm. The ratio of these two emission intensities ( $I_{576}/I_{442}$ ) holds to a good linear relationship, with  $R^2$  value of 0.999 (Fig. S3, ESI). This linearity was maintained up to 1.2 equiv. of  $[\text{Al}^{3+}]$ , after which point further addition of  $\text{Al}^{3+}$  led to no further increase in emission intensity ratio (Fig S3a, ESI). The large change in  $I_{576}/I_{442}$  (0.1 to 2.5) makes for facile analysis of the ratiometric signal, a further improvement of previous ratiometric  $\text{Al}^{3+}$  sensors. The LOD of TPRH for  $\text{Al}^{3+}$  was estimated from the fluorescence titration<sup>25</sup> to be  $6.7 \times 10^{-8}$  M (Fig S4, ESI).

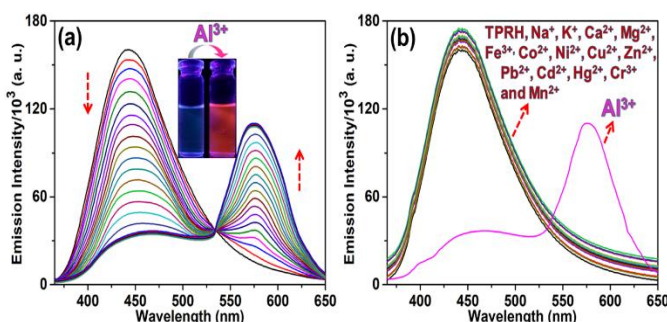


**Figure 2:** (a) Change of emission spectra of TPRH upon gradual addition of  $\text{Al}^{3+}$  (0 to 1.5 equivalents). (b) Changes of emission spectra of TPRH upon addition of 5 equivalents of stated guest analytes. TPRH (20  $\mu\text{M}$ ) in MeOH/ $\text{H}_2\text{O}$  (1/4, v/v), HEPES buffer (10 mM), pH 7.2, 25  $^\circ\text{C}$ ,  $\lambda_{\text{ex}} = 350$  nm.

In order to gain a deeper insight into the stoichiometry of  $\text{Al}^{3+}$  binding with TPRH, a Job's plot experiment was performed by combining solutions of  $\text{AlCl}_3$  and TPRH in varying molar ratios and measuring fluorescence emission ratio (Fig S5, ESI). From the Job's plot, a 1:1 binding stoichiometry was determined between TPRH and  $\text{Al}^{3+}$ . Mass spectrometry (HRMS<sup>+</sup>) adds further support to 1:1 binding, with the observation of a peak at  $m/z$  926.26, corresponding to the molecular weight of  $[\text{TPRH} + \text{Al}^{3+} + 3\text{H}_2\text{O} + 3^{35}\text{Cl}^- + \text{H}^+]^+$  (Fig. S14, ESI).  $^1\text{H}$  NMR titration experiment of TPRH in the presence of  $\text{Al}^{3+}$  was also performed, which establish the interaction between TPRH and  $\text{Al}^{3+}$  (Fig. S15, ESI). The selectivity of TPRH was investigated by fluorescence emission. Addition of a range of metal cations ( $\text{Na}^+$ ,  $\text{K}^+$ ,  $\text{Ca}^{2+}$ ,  $\text{Mg}^{2+}$ ,  $\text{Fe}^{3+}$ ,  $\text{Co}^{2+}$ ,  $\text{Ni}^{2+}$ ,  $\text{Cu}^{2+}$ ,  $\text{Zn}^{2+}$ ,  $\text{Pb}^{2+}$ ,  $\text{Cd}^{2+}$ ,  $\text{Hg}^{2+}$ ,  $\text{Ni}^{2+}$ ,  $\text{Cr}^{3+}$  and  $\text{Mn}^{2+}$ ) to a solution of TPRH gave very little change in fluorescence emission and no species gave rise to the characteristic emission band at 576 nm, indicative of spirolactam ring opening (Fig 2b).

Furthermore, in a competition assay, a solution of TPRH and  $\text{Al}^{3+}$  was prepared and potential competitor metal ions were added (5 equivalents). The emission at 576 nm was monitored and showed that no competitor ion was able to significantly perturb the observed fluorescence, indicating that the TPRH: $\text{Al}^{3+}$

complex is stable towards competing ions (Fig. 3). Taken together, these results demonstrate that TPRH has great potential as a selective  $\text{Al}^{3+}$  sensor, with high levels of sensitivity.

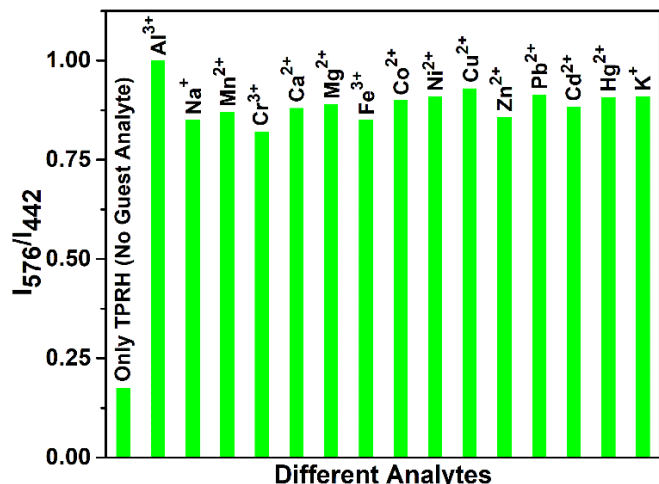


**Figure 3:** A comparative study of emission intensity after the addition of different analytes (5 equivalents) in the solution of TPRH (20  $\mu\text{M}$ ) in presence of  $\text{Al}^{3+}$  (2 equivalents). MeOH/ $\text{H}_2\text{O}$  (1/4, v/v) solution, HEPES buffer (10 mM), pH 7.2, 25  $^\circ\text{C}$ ,  $\lambda_{\text{ex}}$  = 350 nm.

#### pH study

In order to investigate the applicability of the probe in biological and environmental applications, the pH dependence of TPRH was examined, using fluorescence titration. A solution of TPRH was monitored by fluorescence as the pH was adjusted from pH 1 to pH 12, using HCl and NaOH solutions (Fig. 4).

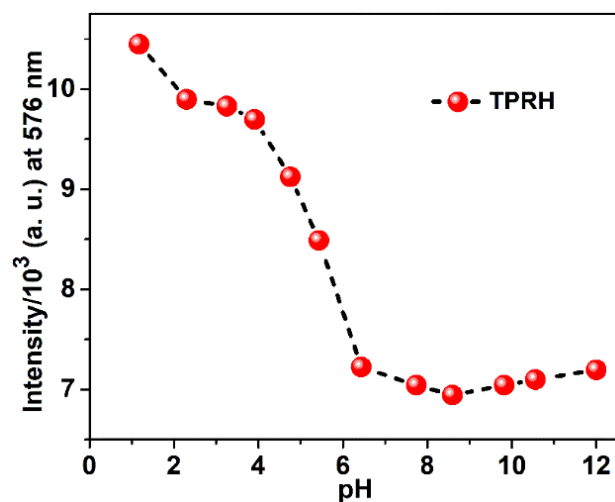


**Figure 4:** Fluorescence response of TPRH at 576 nm (20  $\mu\text{M}$ ,  $\lambda_{\text{ex}}$  = 350 nm) as a function of pH in  $\text{CH}_3\text{OH}-\text{H}_2\text{O}$  (1 : 4, v/v, 25  $^\circ\text{C}$ ); the pH is adjusted by using aqueous solutions of 1 M HCl or 1 M NaOH.

It was found that the probe is sensitive to acidic medium, with an increase in fluorescence observed below pH 6, likely due to acid catalysed ring opening. In neutral and alkali solution, the probe is stable and not sensitive to pH changes, highlighting the potential for this probe to be useful in biological and environmental applications, where pH > 6 is typically encountered. These results indicate that the probe can be used in basic, near-neutral and slight acidic condition, but at lower pH, the spiro-lactam ring opens even in absence of  $\text{Al}^{3+}$  due to

protonation. The probe stable in pH greater than pH 6.2, which is found in the majority of cellular applications. At lower pH, there is pH interference, which we acknowledge in the manuscript. Our continued work in this area looks at developing probes that can operate throughout the pH scale, but this has not been achieved yet. Despite this, operation in pH range 6.2 – 12 allows successful measurement in most applications.

#### Reversibility Study

An essential feature of any chemosensor is its ability to be reversible in its sensing. To test reversibility, a solution of TPRH: $\text{Al}^{3+}$  complex was prepared and  $\text{Na}_2\text{EDTA}$  solution was added incrementally (Fig. 5). Upon addition of  $\text{Na}_2\text{EDTA}$ , the pink-red colour of TPRH- $\text{Al}^{3+}$  was gradually discharged until a colourless solution was observed. In the fluorescence spectrum, as EDTA was added, the emission intensity at 576 nm gradually decreased and restoration of the original peak of TPRH was observed at 442 nm (Fig. 5).

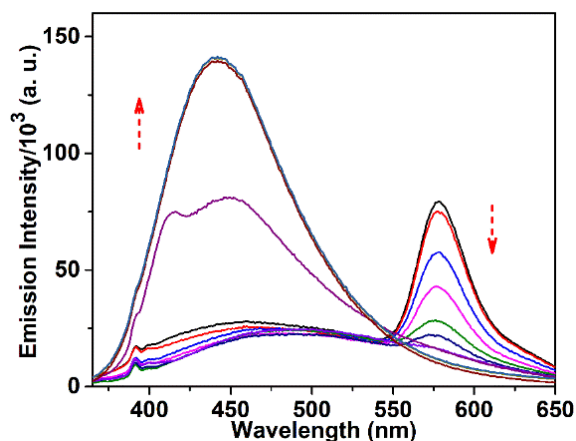


**Figure 5:** Fluorescence titration spectra of TPRH- $\text{Al}^{3+}$  (10  $\mu\text{M}$ ) upon increasing the concentration of  $\text{Na}_2\text{EDTA}$  (0 to 6 equivalents). In MeOH/ $\text{H}_2\text{O}$  (1/4, v/v) solution, HEPES buffer (10 mM), pH 7.2, 25  $^\circ\text{C}$ ,  $\lambda_{\text{ex}}$  = 350 nm.

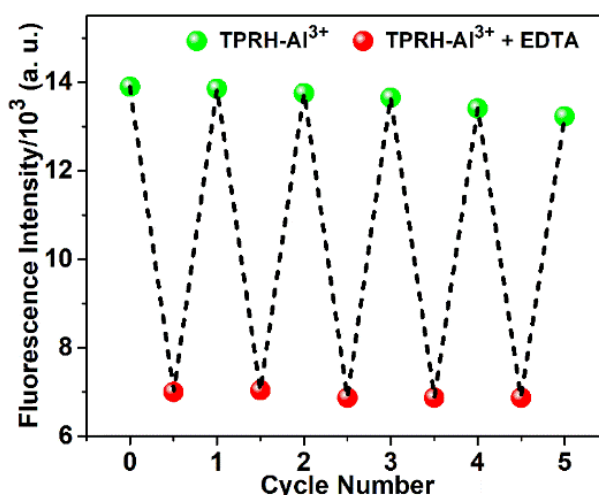


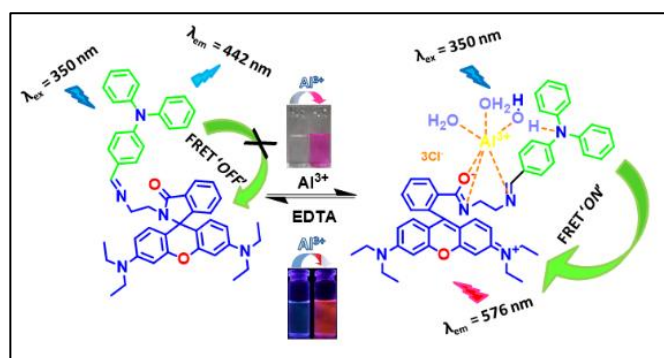
**Figure 6:** The fluorescent "ON-OFF" cycles of TPRH at 576 nm upon alternation addition of  $\text{Al}^{3+}$  and EDTA in mixed aqueous medium. TPRH (10  $\mu\text{M}$ ) in MeOH/ $\text{H}_2\text{O}$  (1/4, v/v), HEPES buffer (10 mM), pH 7.2, 25  $^\circ\text{C}$ .

This indicates that the stability of the TPRH- $\text{Al}^{3+}$  complex is lower than the  $\text{Al-EDTA}$  complex and that the sensing ability of TPRH is reversible. Reversibility was further explored by taking this solution containing EDTA: $\text{Al}^{3+}$  complex and unbound TPRH and adding a second addition of  $\text{Al}^{3+}$ . Upon addition of  $\text{Al}^{3+}$ ,

fluorescence at 576 nm was restored, with disappearance of the peak at 542 nm. Successive cycling of Na<sub>2</sub>EDTA and AlCl<sub>3</sub> was carried out and full reversibility was shown for six cycles, with only around 5% loss of maximum emission and full retention of ratiometric response to Al<sup>3+</sup> (Fig. 6).

### Potential binding mechanism

The chemosensor TPRH contains two potential fluorophores: the triphenylamine and rhodamine-B fragments. These two chromophores, separated by an ethylenediamine linker, have the potential to display fluorescence resonance energy transfer (FRET) when close in space. In the free, unbound state of TPRH, the rhodamine unit sits in the spirolactam form. With an excitation wavelength of 350 nm, light is absorbed and emitted solely by the triphenylamine unit, with no FRET observed. Upon Al<sup>3+</sup> binding, most likely to the hard-acid donors of the imine N and amide O, the spirolactam ring opens and emission is observed at 576 nm, due to FRET between the donor triphenylamine and acceptor rhodamine units.



Scheme 3. Proposed FRET-Based Sensing Strategy of TPRH with Al<sup>3+</sup>

Since Al<sup>3+</sup> is facilitating FRET, it is hypothesised that the Al acts to coordinate both rhodamine and triphenylamine units (through a bridging H<sub>2</sub>O), bringing the fluorophores close in space and allowing FRET. The FRET efficiency was calculated to be 44% for the aluminium-bound complex (see ESI, Fig. S6). As a result of the FRET process, emission is observed from the rhodamine unit at 576 nm and ratiometric analysis of the emissions at 576 nm and 542 nm allows for Al<sup>3+</sup> quantification. The origin of selectivity towards Al<sup>3+</sup> over other metal cations is not clear at this stage, but may be due to the size of binding cavity provided by the rhodamine and triphenylamine units. Scheme 3 shows the postulated binding mechanism of the probe TPRH with Al<sup>3+</sup>.

### Cytotoxic effects of the probe and its Al<sup>3+</sup> Complex

Cell viability was represented in Figure 7; where up to 50 μM concentrations of TPRH shows around 56.67% (without Al<sup>3+</sup>) & 53.22% (with 10 μM Al<sup>3+</sup>) of viable cells respectively predicting it is a safe probe to use in a biological system. We have used 10 μM TPRH solutions for imaging which shows high number of viable cells (86.88% without Al<sup>3+</sup> and 81.23% with Al<sup>3+</sup>) concluding its nontoxic nature. Cell viability was calculated using the following calculation:

$$\% \text{ of Cell Viability} = \frac{(\text{Absorbance of treatment group} - \text{blank})}{(\text{Absorbance of control group} - \text{blank})} \times 100$$

TPRH has good cell permeability as well as stability at biological pH (7.4). Our MTT data indicates its safe and non-toxic nature towards cell. It does not cause cell damages such as swelling or lysis. TPRH is highly sensitive towards Al<sup>3+</sup> and a dose as low as 10 μM can be easily detected by fluorescence microscopy. Therefore, this fluorescence probe is safe and non-toxic to use for biological samples to detect Al<sup>3+</sup>.

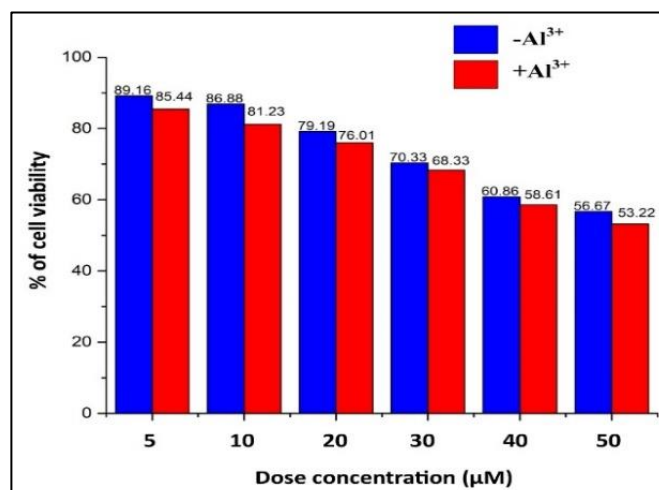


Figure 7: Percentage of viable human peripheral blood mononuclear cells (PBMCs) over TPRH concentration range (5–50 μM) in presence and absence of Al<sup>3+</sup>. Cells were incubated for 30 minutes at 37°C in dark.

### Bioimaging

An ideal approach for designing the experiments would be conducting the bioimaging on both primary cells and secondary cell lines. Since, primary cells are more sensitive and represent a biological system more accurately than secondary cell lines, we designed this study on primary human PBMCs.

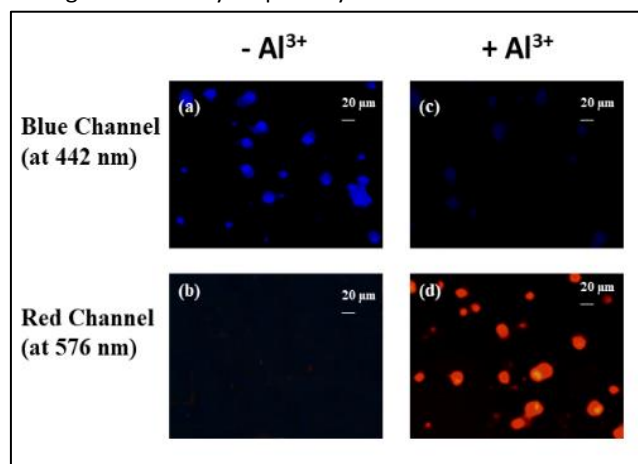
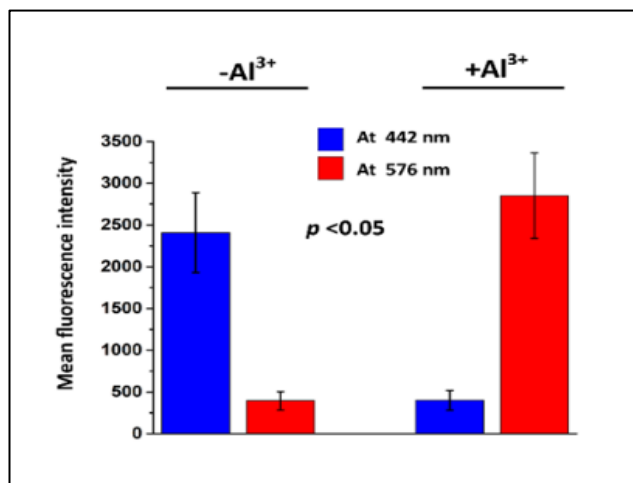


Figure 8: Fluorescence images (40x) of human PBMCs treated with (c, d) and without (a, b) Al<sup>3+</sup> (10 μM) along with 10 μM TPRH. Images were taken at blue (emission at 442nm) and red channel (emission at 576nm) channel. λ<sub>ex</sub> = 350 nm. TPRH (10 μM) could successfully detect Al<sup>3+</sup> in cells and the fluorescence has shifted from blue to red. Whereas without Al<sup>3+</sup> no significant red signals were detected.

Although replicating this experiment on cell lines may add more insights for comparison, but that was our limitation. Figure 8 depicts the fluorescence images of human PBMCs treated with and without  $\text{Al}^{3+}$  (10  $\mu\text{M}$ ) in combination with 10  $\mu\text{M}$  TPRH. Here, the cells exhibit a significant blue fluorescence and very little or no red fluorescence (Fig. 8a & b respectively), when treated with only TPRH and without  $\text{Al}^{3+}$ , but, remarkably, after addition of  $\text{Al}^{3+}$  shows a distinct red intensity, with considerably redundant blue intensity (Fig. 8c & d respectively), indicating the interactions between TPRH and  $\text{Al}^{3+}$ .

The size chart for the cells is also given (20  $\mu\text{m}$ ) in Figure 9. At blue channel (at 442 nm), TPRH has shown sharp intensities ( $2408 \pm 477.3$ ) when the cells were  $\text{Al}^{3+}$  untreated. At red channel (at 576nm) almost negligible fluorescence intensities were found ( $396 \pm 109.9$ ) for  $\text{Al}^{3+}$  untreated samples. However, when  $\text{Al}^{3+}$  was added significant increase ( $p < 0.05$ ) in red fluorescence ( $2851 \pm 511.6$ ) was observed. The blue fluorescence got significantly ( $p < 0.05$ ) diminished ( $401 \pm 117.7$ ) after addition of  $\text{Al}^{3+}$ . These results strongly suggest that TPRH is a precise and convenient fluorescent probe to measure  $\text{Al}^{3+}$  in biological system.



**Figure 9:** The mean fluorescence intensities were measured in ImageJ, which shows a significant ( $p < 0.05$ ) shifts from blue ( $401 \pm 117.7$ ) to red ( $2851 \pm 511.6$ ) fluorescence, when  $\text{Al}^{3+}$  was added. When there was no  $\text{Al}^{3+}$  present blue fluorescence ( $2408 \pm 477.3$ ) was significantly ( $p < 0.05$ ) more visible than the red ( $396 \pm 109.9$ ). The fluorescence intensity of individual cell was measured (15 cells per condition) and statistics were done in Origin Pro 9 software.

### Solid state dipstick device

Prompted by the success in the development of TPRH as a selective  $\text{Al}^{3+}$  sensor, we resolved to fabricate a simple device for detecting  $\text{Al}^{3+}$ . For this application, we decided to use a simple dipstick method, in which a test strip (silica TLC plate) was immersed in a solution of TPRH (0.1 mM, MeOH: H<sub>2</sub>O 1:4) and then left to dry in air. When these strips are again immersed into a solution of  $\text{Al}^{3+}$  (0.01mM), a prominent change of colour can easily be seen by the naked eye (colourless to pink-red, Fig. 10a) and when exposed to hand-held 365 nm UV light, a clear change in emitted light is observed (Fig. 10b). The distinct colour change allows for a quick and easy method for qualitative detection of  $\text{Al}^{3+}$ , without the need for any expensive spectrometers. With further development, a similar device could be used for real-time aluminium detection in field studies.

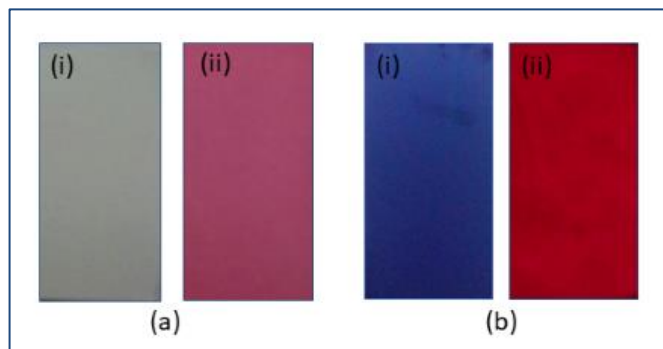


**Figure 10:** Colour changes of TPRH on test paper in the (i) absence and (ii) presence of  $\text{Al}^{3+}$  (a) under ambient light and (b) hand held 365 nm UV light, respectively.

### Molecular logic gate

Logic gates can be used as fundamental microdevices for electronic components. Logic gates have been produced that incorporate small molecules as inputs with fluorescence outputs.<sup>26</sup> There are 16 different types of logic gates that can be produced from two inputs and one output.<sup>27</sup> In this work, we have produced an INHIBIT logic gate, based on the two inputs  $\text{Al}^{3+}$  and EDTA with the fluorescence emission at 576 nm as an output. This combination follows an INHIBIT truth table (Table S1, ESI). This logic gate system is generally represented with Boolean algebra using binary code 0 and 1. This '0' represents the fluorescence property for an inactive state 'NO'/'OFF' and '1' stands for active state 'YES'/'ON' of the probe TPRH. The results of this study show that in the absence of any chemical input (no guest analyte), TPRH shows no noticeable emission at 576 nm, i.e. output 0 (OFF/NO-state). Addition of INPUT 1 ( $\text{Al}^{3+}$ ) gives a prominent fluorescence at 576 nm, i.e., the output 1 (ON/YES-state). Application of both INPUT 1 and INPUT 2 (EDTA) together showed no visible fluorescence at 576 nm, i.e., output 0 (OFF/NO-state).

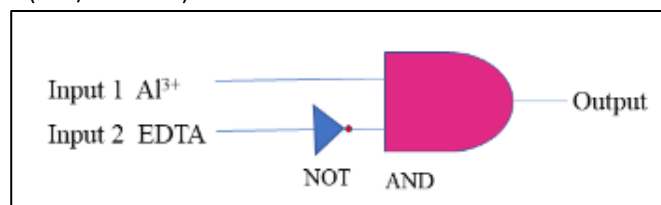


**Figure 11:** General representation of the 'INHIBIT' logic gate.

This system represents an INHIBIT logic gate for TPRH, which is depicted in Figure 11. These results show a system that mimics the functions of a semiconductor logic gate, where fluorescence emission spectroscopy is one of the most important techniques to monitor the output at the molecular level. The applicability of TPRH as a keypad lock sensing device for  $\text{Al}^{3+}$ . Thus, with the alteration of the order of chemical inputs the output intensity signals changed which suggested the use of probe 1 as a potential molecular keypad lock that could be unlocked only by applying the chemical inputs sequentially such as  $\text{TPRH} \rightarrow \text{Al}^{3+} \rightarrow \text{'FRET-ON'}$ , while the reverse entries of  $\text{TPRH} \rightarrow \text{Al}^{3+} \rightarrow \text{EDTA} \rightarrow \text{'FRET-off'}$  and other possible combinations maintained the 'turn-Off' state.

## Experimental

### General:

Chemicals and solvents were purchased from Sigma-Aldrich and used without further purification. Silica gel (100-200 mesh, Merck) was used for column chromatography. NMR spectra were recorded on a Varian VXR-400 spectrometer ( $^1\text{H}$  at 399.97 Hz,  $^{13}\text{C}$  at 100.57 MHz) at 295 K in commercially available  $d^6$  DMSO, with TMS as an internal standard. Chemical shifts are expressed in  $\delta$  units and coupling constants in Hz. UV-Vis spectra were recorded using a Cary 5000 high performance UV-Vis-NIR spectrophotometer, controlled by Cary WinUV software. Fluorescence was recorded using a Horiba Fluorolog-3 spectrometer using FluorEssence software.

### General method of UV-Vis absorption and fluorescence emission titrations:

For both UV-Vis and fluorescence titrations, a stock solution of TPRH was prepared (20  $\mu\text{M}$ ) in  $\text{CH}_3\text{OH-H}_2\text{O}$  (1:4, v/v) in the presence of HEPES buffer (10 mM) solution at pH = 7.2. The solution of the guest cations using their perchlorate/chloride salts at 20  $\mu\text{M}$  were prepared in buffered deionised water at pH 7.2. The absorption spectra of these solutions were recorded by means of UV-Vis methods using a 10 mm pathlength quartz cuvette. Fluorescence emission was measured in a 10 mm pathlength quartz cuvette with the excitation wavelength 350 nm.

### Synthesis of compound 1 (4-(((2-aminoethyl)imino)methyl)-N,N-diphenylaniline):

Ethylene diamine (150 mg, 2.5 mmol) was added to the stirred solution of 4-(diphenylamino)benzaldehyde (546 mg, 2 mmol) in dry ethanol solvent (10 ml) and the mixture was refluxed for 4 hours. The mixture was cooled to room temperature and was poured into cold water. The precipitation that formed was collected through filtration and dried under vacuum. This crude material was purified by column chromatography on silica using 5% ethyl acetate in petroleum ether as eluent. Yield: 480 mg (72%).  $^1\text{H}$  NMR (400 MHz,  $\text{CDCl}_3$ ):  $\delta$  2.88 (t, J = 5.2 Hz, 2H,  $\text{CH}_2$ ), 3.64 (t, J = 5.2 Hz, 2H,  $\text{CH}_2$ ), 4.95 (s, 2H,  $\text{NH}_2$ ), 7.14 – 7.31 (m, 4H, Ar), 7.51 – 7.56 (m, 5H, Ar), 7.58 – 7.63 (m, 5H, Ar), 8.22 (s, 1H,  $\text{CH}=\text{N}$ ).  $^{13}\text{C}$  NMR (75 MHz,  $\text{CDCl}_3$ ):  $\delta$  55.6, 59.9, 122.1, 124.0, 126.4, 126.8, 128.2, 130.4, 148.8, 150.6, 161.5.

MS (ESI, positive mode): calcd for  $\text{C}_{21}\text{H}_{21}\text{N}_3$   $[\text{M}+\text{H}]^+$  (m/z): 316.18; found: 316.13.

### Synthesis of TPRH (3',6'-bis(diethylamino)-2-(2-((4-(diphenylamino)benzylidene)amino)ethyl)spiro[isoindoline 1,9'-xanthen]-3-one):

A mixture of 4-(((2-aminoethyl)imino)methyl)-N,N-diphenylaniline (**1**) (315 mg, 1.00 mmol) and N-(9-(2-(chlorocarbonyl)phenyl)-6-(ethylamino)-3H-xanthen-3-ylidene)-N-ethylethanaminium chloride (**2**) (468 mg, 1.00 mmol) in anhydrous acetonitrile (20 ml) was heated at reflux for 12 h. The solvent was removed under reduced pressure to give a yellow residue, which was purified by column chromatography (silica gel, 5% ethyl acetate in petroleum ether) to give TPRH as a crystalline solid (530 mg, 70%).  $^1\text{H}$  NMR (400 MHz,  $d^6$ -DMSO):  $\delta$  1.08 (t, J = 6.5 Hz, 12H,  $\text{CH}_3$ ), 2.46 – 2.42

(m, 8H,  $\text{CH}_2\text{CH}_2$ ), 3.20 – 3.40 (m, 8H,  $\text{CH}_2\text{CH}_3$ ), 6.30 – 6.40 (m, 6H, Ar (*rhodamine*)), 6.87 (d, 2H, J = 6.5 Hz, N=CH-Ar-NPh<sub>2</sub>), 7.00 – 7.30 (m, 1H, Ar (*rhodamine*)), 7.05 (d, 4H, J = 6.0 Hz, NPh<sub>2</sub> (*ortho-H*)), 7.11 (t, 2H, J = 6.0 Hz, NPh<sub>2</sub> (*para-H*)), 7.33 (t, 4H, J = 6.0 Hz, NPh<sub>2</sub> (*meta-H*)), 7.46 (d, 2H, J = 6.5 Hz, N=CH-Ar-NPh<sub>2</sub>), 7.48 – 7.54 (m, 2H, Ar (*rhodamine*)), 7.76 – 7.82 (m, 1H, Ar (*rhodamine*)), 7.86 (s, 1H,  $\text{CH}=\text{N}$ ).  $^{13}\text{C}$  NMR (100 MHz,  $\text{CDCl}_3$ ):  $\delta$  12.6, 30.9, 44.3, 58.9, 64.9, 97.8, 105.5, 108.0, 121.8, 122.6, 123.6, 123.7, 125.1, 126.3, 127.9, 128.9, 129.0, 129.3, 129.5, 129.7, 131.0, 132.3, 147.1, 148.7, 149.9, 153.3, 153.7, 161.9, 168.2, 207.1. HRMS (ESI, positive mode): calcd for  $\text{C}_{49}\text{H}_{49}\text{N}_5\text{O}_2$   $[\text{M}+\text{H}]^+$  (m/z): 740.3959; found: 740.3968.

### $\text{Al}^{3+}$ complex of TPRH

The receptor, TPRH (50 mg, 0.07 mmol) and  $\text{AlCl}_3$  (12 mg, 0.09 mmol) were dissolved in methanol (7 ml) and the mixture heated to reflux for 10 h. The reaction mixture was cooled to room temperature and a red precipitate formed, which was collected by filtration and dried in vacuum to give the title compound. MS (ESI, Positive mode): calcd. for  $\text{C}_{49}\text{H}_{56}\text{AlCl}_3\text{N}_5\text{O}_5$   $[\text{TPRH} + \text{Al}^{3+} + 3^{35}\text{Cl}^- + 3\text{H}_2\text{O} + \text{H}^+]^+$  (m/z): 926.31; found: 926.26.

### Details of bio-imaging

#### Materials Methods

Venous blood (3ml) was obtained from a healthy, male, volunteer donor (age - 30 years) with his informed consent. Peripheral blood mononuclear cells (PBMCs) were harvested by density gradient centrifugation utilizing histopaque-1077 gradient [SIGMA]. PBMCs were washed twice with ice cold PBS and then suspended in the same. Suspended cells were treated with [10  $\mu\text{M}$   $\text{AlCl}_3$ ] and without  $\text{Al}^{3+}$  (control vehicle). TPRH samples were prepared in PBS containing 0.5% DMSO. Both  $\text{Al}^{3+}$  treated and untreated samples were incubated with 10  $\mu\text{M}$  TPRH solutions for 30 minutes at 37°C in dark. Intracellular fluorescence intensity was detected by fluorescence microscope (Carl Zeiss HBO 100) under 40X magnification with fluorescence emissions at 442nm (Blue channel, Filter set 49) nm and 576 nm (Red channel, Filter Set 42), respectively. Relative fluorescence intensities were calculated using ImageJ software.

#### MTT assay

To determine cell viability against TPRH, PBMCs were treated with different concentrations of TPRH solution (5-50  $\mu\text{M}$ ) with or without  $\text{Al}^{3+}$  (10  $\mu\text{M}$ ) for 1 hour at 37°C against control cell suspension without TPRH. Cell density remained 0.05 x 10<sup>6</sup> cells per well in a 96- well plate. 100  $\mu\text{l}$  of MTT solution (5 mg/ml) was added to each well including control and incubated for 4 hours at 37°C. The purple coloured formazan crystals were dissolved with 100  $\mu\text{l}$  DMSO and the absorbance were measured at 570 nm. Cell viability was calculated using the

$$\% \text{ of Cell Viability} = \frac{(\text{Absorbance of treatment group} - \text{blank})}{(\text{Absorbance of control group} - \text{blank})} \times 100$$

following calculation:

## Conclusions

In summary, we have developed a new triphenylamine and rhodamine-B based chemosensor, which can exclusively detect  $Al^{3+}$  via ratiometric fluorescence response. The selective detection of  $Al^{3+}$  by ratiometric analysis of two emission wavelengths is important as it allows measurement without needing to know the probe concentration and is not susceptible to interference by competitor ions. Ratiometric analysis removes issues of quenching by unknown contaminants. The probe, TPRH shows excellent selectivity to  $Al^{3+}$  over a broad range of competitor metal ions, shows reversible binding for at least six cycles and has a limit of detection of  $10^{-8}$  M. To probe some potential applications, a solid state device was produced that gives on response in the presence of solutions containing  $Al^{3+}$  and an INHIBIT logic gate was generated. Furthermore, the probe was tested in a range of water samples and successfully showed elevated aluminium levels in contaminated water sources. Overall, this new probe has the long term potential to improve health and wellbeing by sensing toxic metal in water samples in an accurate and effective manner. TPRH can even serve as an excellent probe to detect  $Al^{3+}$  in biological system (such as cells) in a nontoxic and convenient way.

#### Conflicts of interest

There are no conflicts to declare.

#### Acknowledgements

S.Das Acknowledges Newton International Fellowships Royal Society (UK) for fellowship (ref: NIF\R1\182209).

#### Notes and references

- 1 Y. M. You, Y. J. Han, Y. M. Lee, S. Y. Park, W. W. Nam and S. J. Lippard, *J. Am. Chem. Soc.*, 2011, **133**, 11488.
- 2 J. Han, X. Tang, Y. Wang, R. J. Liu, L. Wang and L. Ni, *Spectrochim. Acta, Part A*, 2018, **205**, 597–602.
- 3 H. H. Wang, Q. Gan, X. J. Wang, L. Xue, S. H. Liu and H. Jiang, *Org. Lett.*, 2007, **9**, 4995.
- 4 B. Qiao, S. G. Sun, N. Jiang, S. Zhang and X. J. Peng, *Dalton Trans.*, 2014, **43**, 4626.
- 5 E. Ranyuk, C. M. Douaihy, A. Bessmertnykh, F. Denat, A. Averin, I. Beletskaya and R. Guillard, *Org. Lett.*, 2009, **11**, 987.
- 6 M. Zhang, Y. Yang, L. Y. Liu, W. X. Chang and J. Li, *Macromolecules*, 2016, **49**, 844.
- 7 M. Shyamal, P. Mazumdar, S. Maity, G. P. Sahoo, G. Salgado-Morán and A. Misra, *J. Phys. Chem. A*, 2016, **120**, 210.
- 8 D. P. Perl and A. R. Brody, *Science*, 1980, **208**, 297.
- 9 D. P. Perl, D. C. Gajdusek, R. M. Garruto, R. T. Yanagihara, C. J. Gibbs, *Science*, 1982, **217**, 1053.
- 10 A. Lankoff, A. Banasik, A. Duma, D. Ochniak, H. Lisowska, T. Kuszewski, S. Gózdź and A. Wojcik, *Toxicol. Lett.*, 2006, **161**, 27.
- 11 J. Savory, R. L. Bertholf, M. R. Wills, *Aluminium toxicity in chronic renal insufficiency. Clin. Endocrinol. Metab.* 1985, **14**, 681–702.
- 12 (a) P. Nayak, *Environ. Res.*, 2002, **89**, 101–115, (b) N. Fimreite, O. O. Hansen and H. C. Pettersen, *Bull. Environ. Contam. Toxicol.*, 1997, **58**, 1–7.
- 13 (a) T. Han, X. Feng, B. Tong, J. Shi, L. Chen, J. Zhi and Y. Dong, *Chem. Commun.*, 2012, **48**, 416–418; (b) Z. Krejpcio and R. W. Wojciak, *Pol. J. Environ. Stud.*, 2002, **11**, 251–254; (c) J. Barcelo and C. Poschenrieder, *Environ. Exp. Bot.*, 2002, **48**, 75–92; (d) T. Han, X. Feng, B. Tong, J. Shi, L. Chen, J. Zhi and Y. Dong, *Chem. Commun.*, 2012, **48**, 416–418.
- 14 (a) S. Das, M. Dutta and D. Das, *Anal. Methods*, 2013, **5**, 6262–6285; (b) D. Maity and T. Govindaraju, *Eur. J. Inorg. Chem.*, 2011, 5479–5485; (c) J.-C. Qin, X. Cheng, R. Fang, M. Wang, Z. Yang, T. Li and Y. Li, *Spectrochim. Acta, Part A*, 2016, **152**, 352–357; (d) L. McDonald, J. Wang, N. Alexander, H. Li, T. Liu and Y. Pang, *J. Phys. Chem. B*, 2016, **120**, 766–772; (e) G. R. Zou, C. X. Liu, C. Cong, Z. T. Fang, W. Yang, X. M. Luo, S. K. Jia, F. Wu and X. Zhou, *Chem. Commun.*, 2018, 54, 13107–13110; (f) B. Naskar, A. Bauzá, A. Frontera, D. K. Maiti, C. D. Mukhopadhyay and S. Goswami, *Dalton Trans.*, 2018, 47, 15907–15916; (g) A. Sahana, A. Banerjee, S. Lohar, B. Sarkar, S. K. Mukhopadhyay, and D. Das, *Inorg. Chem.*, 2013, **52**, 3627–3633.
- 15 Z. Li, W. Chen, L. Dong, Y. Song, R. Li, Q. Li, D. Qu, H. Zhang, Q. Yang and Y. Li, *New J. Chem.*, 2020, **44**, 3261–3267; (b) X. Sun, Y.-W. Wang and Y. Peng, *Org. Lett.*, 2012, **14**, 3420–3423.
- 16 (a) K. Boonkitpatarakul, J. Wang, N. Niamnont, B. Liu, L. McDonald, Y. Pang and M. Sukwattanasinitt, *ACS Sens.*, 2015, **1**, 144–150; (b) X. Sun, Y.-W. Wang and Y. Peng, *Org. Lett.*, 2012, **14**, 3420–3423; (c) H. Y. Liu, T. Q. Liu, J. Li, Y. M. Zhang, J. H. Li, J. Song, J. L. Qu and W. Y. Wong, *J. Mater. Chem. B*, 2018, 6, 5435–5442. (d) B. Sen, S. Pal, S. Lohar, M. Mukherjee, S. K. Mandal, A. R. Khuda-Bukhsh and P. Chattopadhyay, *RSC Adv.*, 2014, **4**, 21471; (e) A. Manna, D. Sain, N. Guchhaita and S. Goswami, *New J. Chem.*, 2017, **41**, 14266; (f) H. Liu, T. Liu, J. Li, Y. Zhang, J. Li, J. Song, J. Qu and W.-Y. Wong, *J. Mater. Chem. B*, 2018, **6**, 5435–5442; (g) A. E. Sadak and E. Karakuş, *J. Fluoresc.*, 2020, **30**, 213–220.
- 17 (a) A. Roy, S. Dey, P. Roy, *Sens. Actuators B Chem.*, 2016, **237**, 628; (b) H. Xie, Y. Wu, J. Huang, F. Zeng, H. Wu, X. Xia, C. Yu, S. Wu, *Talanta*, 2016, **151**, 8; (c) Y. Zhang, Y. Fang, N.-Z. Xu, M.-Q. Zhang, G.-Z. Wu, C. Yao, *Chin. Chem. Lett.*, 2016, **27**, 1673; (d) D. Jeyanthi, M. Iniya, K. Krishnaveni, D. Chellappa, *RSC Adv.*, 2013, **3**, 20984; (e) J.-c. Qin, Z.-y. Yang, *Anal. Methods*, 2015, **7**, 2036; (f) S. Sinha, B. Chowdhury, P. Ghosh, *Inorganic Chemistry*, 2016, **55**, 9212; (g) S. Goswami, A. Manna, S. Paul, AK Maity, P Saha, CK Quah, HK Fun, *RSC Advances*, 2014, **3**, 34572.
- 18 (a) J. Fan, M. Hu, P. Zhan and X. Peng, *Chem. Soc. Rev.*, 2013, **42**, 29; (b) N. Kumar, V. Bhalla and M. Kumar, *Analyst*, 2014, **139**, 543; (c) V. Luxami, M. Verma, R. Rani, K. Paul and S. Kumar, *Org. Biomol. Chem.*, 2012, **10**, 8076; (d) A. K. Mandal, M. Suresh, P. Das and A. Das, *Chem.–Eur. J.*, 2012, **18**, 3906; (e) M. Suresh, A. K. Mandal, M. K. Kesharwani, N. N. Adarsh, B. Ganguli, R. K. Kanaparthi, A. Samanta and A. Das, *J. Org. Chem.*, 2011, **76**, 138; (f) H. Yu, Y. Xiao, H. Guo and X. Qian, *Chem.–Eur. J.*, 2011, **17**, 3179; (g) M. Kumar, N. Kumar, V. Bhalla, H. Singh, P. R. Sharma and T. Kaur, *Org. Lett.*, 2011, **13**, 1422; (h) W. Guo, X. Lv, J. Liu, Y. L. Liu, Y. Zhao, M. L. Chen and P. Wang, *Org. Biomol. Chem.*, 2011, **9**, 4954; (i) X. Zhou, F. Su, H. Lu, P. Senechal-Willis, Y. Tian, R. H. Johnson and D. R. Meldrum, *Biomaterials*, 2012, **33**, 171; (j) L. Yuan, W. Lin, Z. Cao, J. Wang and B. Chen, *Chem.–Eur. J.*, 2012, **18**, 1247; (k) W. Y. Lin, L. L. Long, B. B. Chen, W. S. Gao and L. Yuan, *Chem. Commun.*, 2011, **47**, 893; (l) C. Kar, M. D. Adhikari, A. Ramesh and G. Das, *Inorg. Chem.*, 2013, **52**, 743.
- 19 (a) T. Schraderr and A. D. Hamilton, *Functional Synthetic Receptors, Wiley-VCH, Weinheim, Germany*, 2005; (b) J. P. Desvergne, A. Czarnik and W. Kluwer, *Chemosensors of Ion and Molecule Recognition, Dordrecht*, 1997; (c) A. W. Czarnik, *Fluorescent Chemosensors for Ion and Molecule Recognition, American Chemical Society, Washington, DC*, 1992; (d) R. Mainez-Mañez and F. Sancenon, *Chem. Rev.*, 2003, **103**, 4419; (e) P. D. Beer and P. A. Gale, *Angew. Chem., Int. Ed.*, 2001, **40**, 486; (f) A. P. De Silva, H. Q. N. Gunaratne, T.

- Gunnlaugsson, A. J. M. Huxley, C. P. McCoy, J. T. Rademacher and T. E. Rice, *Chem. Rev.*, 1997, **97**, 1515; (g) Z. Li, W. Chen, L. Dong, Y. Song, R. Li, Q. Li, D. Qu, H. Zhang, Q. Yang and Y. Li, *New J. Chem.*, 2020, **44**, 3261-3267.
- 20 (a) U. E. Spichiger-Keller, *Chemical Sensors and Biosensors for Medical and Biological Applications*, Wiley-VCH, Weinheim, Germany, 1998; (b) V. Amendola, L. Fabbrizzi, F. Forti, M. Licchelli, C. Mangano, P. Pallavicini, A. Poggi, D. Sacchi and A. Taglieti, *Coord. Chem. Rev.*, 2006, **250**, 273; (c) K. Rurack and U. Resch-Genger, *Chem. Soc. Rev.*, 2002, **31**, 116; (d) P. T. Srinivasan, T. Viraraghavan and K. S. Subramanian, *Water SA*, 1999, **25**, 47.
- 21 (a) R. Zhang, F. Yan, Y. Huang, D. Kong, Q. Ye, J. Xu and Li Chen, *RSC Adv.*, 2016, **6**, 50732-50760; (b) Y. Zhang, S. Xia, M. Fang, W. Mazi, Y. Zeng, T. Johnston, A. Pap, R. L. Luck and H. Liu, *Chem. Commun.*, 2018, **54**, 7625-7628; (c) H. Izawa, S. Wakizono and J. Ichi Kadokawa, *Chem. Commun.*, 2010, **46**, 6359-6361; (d) Y.-Y. Liang, J. Zhang, H. Cui, Z.-S. Shao, C. Cheng, Y.-B. Wang and H.-S. Wang, *Chem. Commun.*, 2020, **56**, 3183-3186; (e) P.-Y. Wang, X. Luo, L.-L. Yang, Y.-C. Zhao, R. D., Z. Li and S. Yang, *Chem. Commun.*, 2019, **55**, 7691-7694; (f) C. Zhang, H. Xie, T. Zhan, J. Zhang, B. Chen, Z. Qian, G. Zhang, W. Zhang and J. Zhou, *Chem. Commun.*, 2019, **55**, 9444-9447.
- 22 (a) S. Goswami, S. Das, K. Aich, B. Pakhira, S. Panja, S. Mukherjee, S. Sarkar, *Org. Lett.*, 2013, **15**, 5412-5415; (b) S. Goswami, K. Aich, S. Das, A. K. Das, D. Sarkar, S. Panja, T. K. Mondal, S. Mukhopadhyay, *Chem. Commun.*, 2013, **49**, 10739-10741; (c) S. Goswami, K. Aich, A. K. Das, A. Manna, S. Das, *RSC Adv.*, 2013, **3**, 2412-2416; (d) S. Goswami, K. Aich, S. Das, S. Basu Roy, B. Pakhira, Sabyasachi Sarkar, *RSC Adv.*, 2014, **4**, 14210-14214; (e) S. Goswami, S. Das, K. Aich, D. Sarkar, T. K. Mondal, C. K. Quah, H.-K. Fun, *Dalton Trans.*, 2013, **42**, 15113-15119; (f) L. Patra, S. Das, S. Gharami, K. Aich, T. K. Mondal, *New J. Chem.*, 2018, **42**, 19076-19082; (g) S. Goswami, K. Aich, S. Das, A. K. Das, A. Manna and S. Halder, *Analyst*, 2013, **138**, 1903-1907; (h) S. Goswami, S. Das, K. Aich, D. Sarkar and T.K.Mondal, *Tetrahedron Lett.*, 2014, **55**, 2695-2699; (i) S. Goswami, S. Das and K. Aich, *Tetrahedron Lett.*, 2013, **54**, 4620-4623; (j) S. Goswami, S. Das, K. Aich, P. K. Nandi, K. Ghoshal, C. K. Quah, M. Bhattacharyya, H.-K. Fun and H. A. A. Aziz, *RSC Adv.*, 2014, **4**, 24881-24886; (k) S. Goswami, S. Das, K. Aich, D. Sarkar and T. K. Mondal, *Tetrahedron Lett.*, 2013, **54**, 6892-6896; (l) S. Das, K. Aich, S. Goswami, C. K. Quah and H. K. Fun, *New J. Chem.*, 2016, **40**, 6414-6420; (m) S. Goswami, S. Das and K. Aich, *RSC Adv.*, 2015, **5**, 28996-29001; (n) S. Das, K. Aich, L. Patra, K. Ghoshal, S. Gharami and M. Bhattacharyya, *Tetrahedron Lett.*, 2018, **59**, 1130-1135.
- 23 T. Mallegol, S. Gmouh, M. A. A. Meziane, M. Blanchard-Desce, O. Mongin, *Synthesis*, 2005, **11**, 1771.
- 24 K. Aich, S. Goswami, S. Das, C. D. Mukhopadhyay, C. K. Quah and H.-K. Fun, *Inorg. Chem.* 2015, **54**, 15, 7309-7315.
- 25 (a) M. Shortreed, R. Kopelman, M. Kuhn and B. Hoyland, *Anal. Chem.*, 1996, **68**, 1414; (b) W. Lin, L. Yuan, Z. Cao, Y. Feng and L. Long, *Chem.-Eur. J.*, 2009, **15**, 5096.
- 26 (a) Z.-H. Fu, L.-B. Yan, X. Zhang, F.-F. Zhu, X.-L. Han, J. Fang, Y.-W. Wang and Y. Peng, *Org. Biomol. Chem.*, 2017, **15**, 4115-4121; (b) V. Bojinov and N. Georgiev, *J. Univ. Chem. Technol. Metall.*, 2011, **46**, 3-26; (c) D. C. Magri, G. J. Brown, G. D. McClean and A. P. de Silva, *J. Am. Chem. Soc.*, 2006, **128**, 4950-4951.
- 27 P. Burger, *Digital design: a practical course*, New York: Wiley, New York, 1988.